



1 Frequency of large volcanic eruptions over the past 200,000 years

2
3 Eric W. Wolff¹, Andrea Burke², Laura Crick², Emily A. Doyle¹, Helen M. Innes², Sue H. Mahony³, James
4 W.B. Rae², Mirko Severi⁴ and R. Stephen J. Sparks³

5 ¹Department of Earth Sciences, University of Cambridge, Cambridge CB2 3EQ, United Kingdom

6 ²School of Earth & Environmental Sciences, University of St Andrews, St Andrews, KY16 9AL, United Kingdom

7 ³School of Earth Sciences, University of Bristol, Bristol BS8 1RJ, United Kingdom

8 ⁴Chemistry Department, University of Florence, Sesto F.no (FI) 50019, Italy

9 *Correspondence to:* Eric W. Wolff (ew428@cam.ac.uk)

10 **Abstract.** Volcanic eruptions are the dominant cause of natural variability in climate forcing on timescales up to multidecadal.
11 Large volcanic eruptions lead to global-scale climate effects and influence the carbon cycle on long timescales. However,
12 estimating the frequency of eruptions is challenging. Here we assess the frequency at which eruptions with particular deposition
13 fluxes are observed in the EPICA Dome C ice core over the last 200 kyr. Using S isotope analysis we confirm that most of the
14 largest peaks recorded at Dome C are from stratospheric eruptions. The cumulative frequency through 200 kyr is close to linear
15 suggesting an approximately constant rate of eruptions. There is no evidence for an increase in the rate of events recorded in
16 Antarctica at either of the last two deglaciations. Millennial variability is at the level expected from recording small numbers
17 of eruptions, while multimillennial variability may be partly due to changes in transport efficiency through the Brewer-Dobson
18 circulation. Our record of events with sulfate deposition rates $> 20 \text{ mg m}^{-2}$ and $>50 \text{ mg m}^{-2}$ contains 678 and 75 eruptions
19 respectively over the last 200 kyr. Calibration with data on historic eruptions and analysis of a global Quaternary dataset of
20 terrestrial eruptions indicates that sulfate peaks with deposition rates $> 20 \text{ mg m}^{-2}$ and $>50 \text{ mg m}^{-2}$ correspond to explosive
21 eruptions of magnitude ≥ 6.5 and ≥ 7 respectively. The largest recorded eruption deposited just over 300 mg m^{-2} .

22 1. Introduction

23 Volcanic eruptions can have devastating local effects, and at a global scale they are one of the important natural components
24 of forcing in the climate system (Robock, 2000). The forcing arises from sulfate aerosol that is formed from SO_2 erupted into
25 the stratosphere. On longer timescales the balance between volcanism and weathering controls the CO_2 content of the
26 atmosphere, and changes in volcanic eruption frequency could contribute to the changes in CO_2 concentration observed at
27 glacial terminations (Huybers and Langmuir, 2009). In order to constrain changes in forcing by volcanic aerosol, as well as
28 any role of volcanoes in glacial-interglacial CO_2 change, a key question is whether global eruption rate is steady and, if not,
29 whether any variation is related to climate.

30 There has been much interest in the notion that rates of explosive volcanism have been moderated by processes related to
31 climate change (Kutterolf et al., 2019; Watt et al., 2013). Rates of mantle melting are expected to be affected by glacial cycles:



32 melting of ice caps leads to unloading, enhanced mantle melting and enhanced volcanism (Huybers and Langmuir, 2009; Jull
33 and McKenzie, 1996). Rates of volcanism might also be affected by sea level change (Huybers and Langmuir, 2009; Kutterolf
34 et al., 2019). Over very long timescales, changes in plate tectonics and occurrence of mantle plume volcanism are expected to
35 be reflected in rates of volcanism.

36 Beyond the period of direct historic observations, explosive eruptions are recorded as tephra deposits in terrestrial and marine
37 records, and as both sulfate and occasional tephra deposits in ice cores. Terrestrial tephra deposits give information about
38 location as well as strength and frequency of eruptions (Brown et al., 2014), but they are notoriously difficult to use, and a
39 statistical approach is needed to turn them into useful measures of eruption frequency (Rougier et al., 2018). Tephra in marine
40 cores offers a further opportunity to compile eruption statistics (Mahony et al., 2020), but it is also challenging to compile a
41 record that is unbiased over time and space. Eruptions are also recorded as sulfate deposition in ice cores. While this provides
42 no direct information on the location and magnitude of each eruption, it can be used to log eruptions relevant for climate
43 forcing (Gao et al., 2008; Sigl et al., 2015). There have been only limited investigations (Castellano et al., 2005; Castellano et
44 al., 2004; Cole-Dai et al., 2021; Lin et al., 2022) to estimate volcanic eruption occurrence from ice core data beyond the last
45 2500 years.

46 Although records from both poles may be combined to identify explosive eruptions recorded at both poles (and therefore most
47 likely having reached the stratosphere), the use of Greenland ice core records alone is complicated, because they are dominated
48 by the relatively local input from Icelandic eruptions. Antarctica has rather few local eruptions (notwithstanding an unusual
49 event at the last deglaciation (McConnell et al., 2017)), and so the record of eruptions is likely dominated by those that have
50 reached the stratosphere and have a global climate effect.

51 Eruptions can be logged using spikes in sulfate, or as a surrogate, spikes in the dielectric profile conductance (DEP) or low
52 frequency electrical conductivity (ECM) of ice (Wolff, 2000), both of which respond to acidity in the ice. Such records are
53 available continuously from a number of ice cores on the East Antarctic plateau. Issues of resolution and diffusion mean that
54 the volcanic spikes cannot be reliably observed to the bottom of the cores, but they are clearly identified over at least the last
55 two glacial cycles. This has for example allowed their use to synchronise age models to 128 ka bp between EPICA cores at
56 Dome C (EDC) and Dronning Maud Land (EDML) (Ruth et al., 2007), to 145 ka between EDC and Vostok (Parrenin et al.,
57 2012), and to 216 ka between EDC and Dome F (Fujita et al., 2015).

58 Several issues make it challenging to construct a consistent record of sulfate deposition throughout an ice core. Firstly, there
59 is a background of sulfate from non-volcanic sources (mainly sea salt and marine biogenic). Because this background, and its
60 variability, changes with climate, methods which merely seek outliers (Castellano et al., 2004) risk recording volcanic events
61 depositing a particular amount of sulfate in some climate periods and not in others. Secondly there is a very large amount of
62 variability in the amount of sulfate deposited in the small footprint of snow surface sampled by an ice core (Gautier et al.,
63 2016; Wolff et al., 2005), so that the sulfate signal of individual eruptions in a single core is subject to great uncertainty.



64 Thirdly, Antarctic ice cores will record some eruptions which did not reach the stratosphere but are smaller eruptions of more
65 regional origin. These can in principle be filtered using sulfur isotope analysis to identify mass independent fractionation
66 (Baroni et al., 2008; Burke et al., 2019; Gautier et al., 2019; McConnell et al., 2017; Savarino et al., 2003a).

67 A final issue is related to resolution and diffusion. Snow accumulation rates at the East Antarctic sites mentioned above (Dome
68 Fuji, EDC, Vostok and EDML) vary from 2-6 cm water equivalent at the different sites in the present day and are typically
69 less than 50% of that in the last glacial maximum. Eruption signals are generally recorded above background for only 2-3
70 years. It is therefore essential to use only data with a good depth resolution, and to estimate the flux across the peak and not
71 just at the maximum, which will certainly be modulated by the resolution. Additionally sulfate peaks diffuse with age (Barnes
72 et al., 2003), and we find that volcanic peaks that were just a few years wide on deposition may appear to be 20 years wide in
73 ice of 200 ka age at EDC. This is helpful because it means that, as layers thin with depth, the decreasing age resolution of our
74 measurements is not a limiting factor. However it makes it yet more challenging to identify eruptions of a particular scale in a
75 consistent way, because peaks that stand clearly above background in recent ice diffuse towards the background in older ice.

76 It is also important to be aware that even a perfect record of sulfate deposition events is not easy to convert into a record of
77 eruption magnitude and frequency. In addition to the strength of the eruption, sulfate deposition depends on the sulfur content
78 of the eruption, the latitude of the volcano and atmospheric transport processes (Marshall et al., 2021). Finally, there are
79 difficulties in converting sulfate loading in an ice core to the magnitude (defined by volcanologists as magma mass erupted).
80 Eruption magnitude is only one of several factors that influence sulfate mass released in explosive eruptions (Wallace and
81 Edmonds, 2011).

82 Despite these problems two recent papers (Cole-Dai et al., 2021; Lin et al., 2022) have attempted to assess eruption frequency.
83 One (Cole-Dai et al., 2021) examined the number of eruptions recorded in the WAIS Divide core over the last 11 kyr, observing
84 variability but no trend in eruption rate. A second (Lin et al., 2022) assessed eruption frequencies recorded in both Greenland
85 and Antarctica over the period from 9-60 kyr ago, and compared them with the rates in the last 2 kyr. For Greenland they
86 found relatively constant rates of eruption through time, but with a small increase in frequency of recorded eruptions across
87 the deglaciation (21-9 ka). This is consistent with the idea that the removal of ice from high latitude eruption regions, with a
88 particular emphasis on Iceland (Jull and McKenzie, 1996), would have led to an increased eruption rate recorded in Greenland.
89 For Antarctica, using methods similar to those we describe later, the authors (Lin et al., 2022) found no significant change in
90 eruption rate across the 60 kyr period.

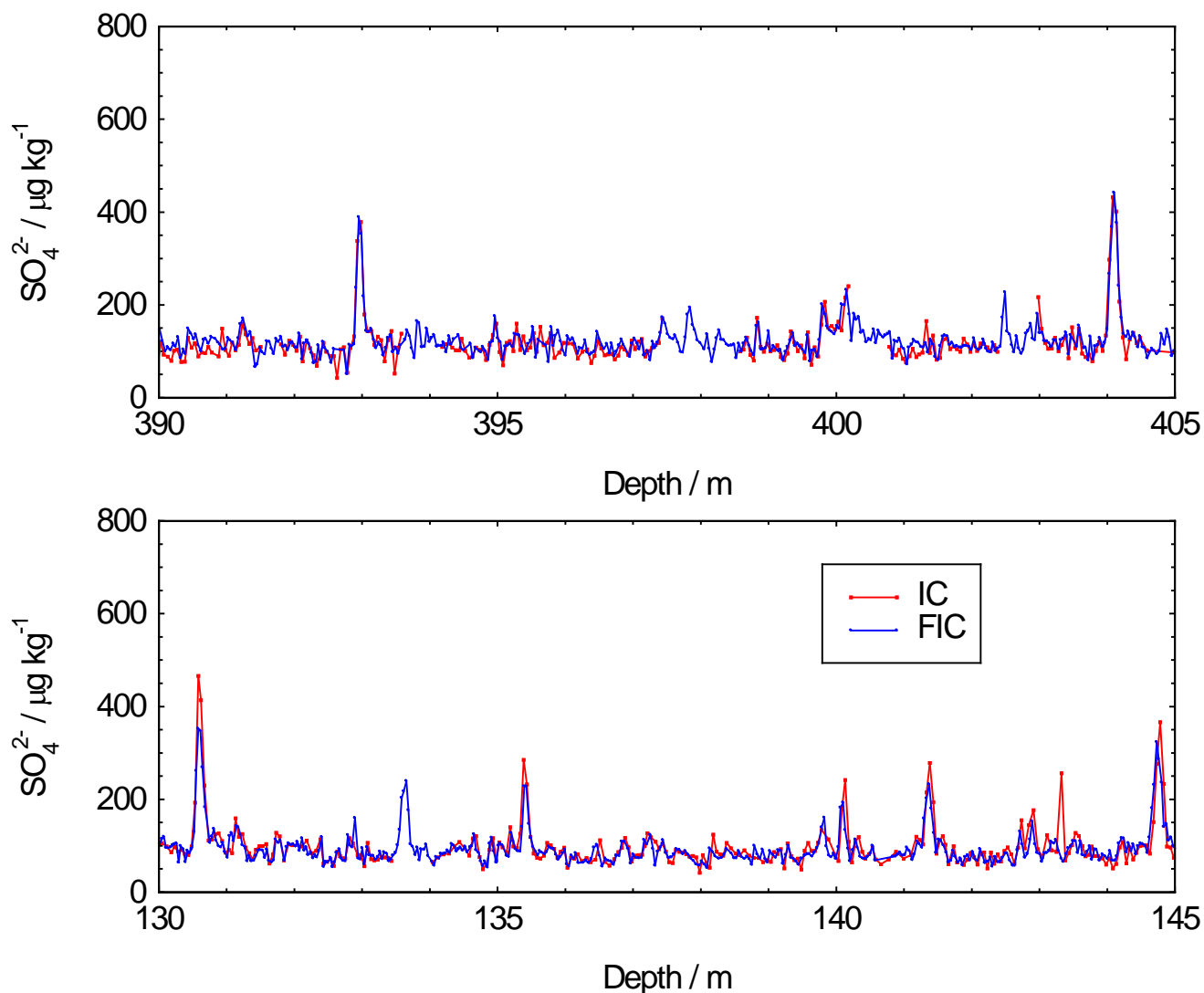
91 In this paper we log eruption frequencies from the Antarctic ice core of EDC to 200 ka, using a methodology that assesses the
92 scale of sulfate deposition consistently with depth, age and climate period.



93 **2. Data**

94 Sulfate was measured along the EPICA Dome C (EDC) ice core by two methods, standard ion chromatography (IC) and fast
95 ion chromatography (FIC) (Littot et al., 2002; Severi et al., 2015). FIC measurements were at higher resolution (typically 5-6
96 cm in the top 100 m, 3-5 cm below that to 770 m, and 2 cm below 770 m) than IC measurements; additionally there are sections
97 of the core where IC data are not available. For these reasons FIC data were preferred.

98 However, although initial tests had suggested good agreement between the methods (Littot et al., 2002), a more detailed
99 analysis suggested some calibration problems during the first field season of FIC use, to a depth of 358.6 metres (11745 years
100 before present (1950) on the AICC2012 age model). In this depth range we consider the well-established IC method to be more
101 reliable. Detailed comparison of FIC and IC data was carried out where both were available. While it is impossible to diagnose
102 exactly what the issue was, a plot of FIC data against IC data for values more than $50 \mu\text{g kg}^{-1}$ above the background showed a
103 gradient of 0.70 for data between 0 and 358.6 m, and 0.94 between 360 m and 720 m. This is shown in Fig. 1 and was used as
104 justification to multiply the FIC values above background (i.e. the residual after subtracting the background) by (1/0.7) for
105 data above 358.6 m (<11.7 ka) during the data processing.

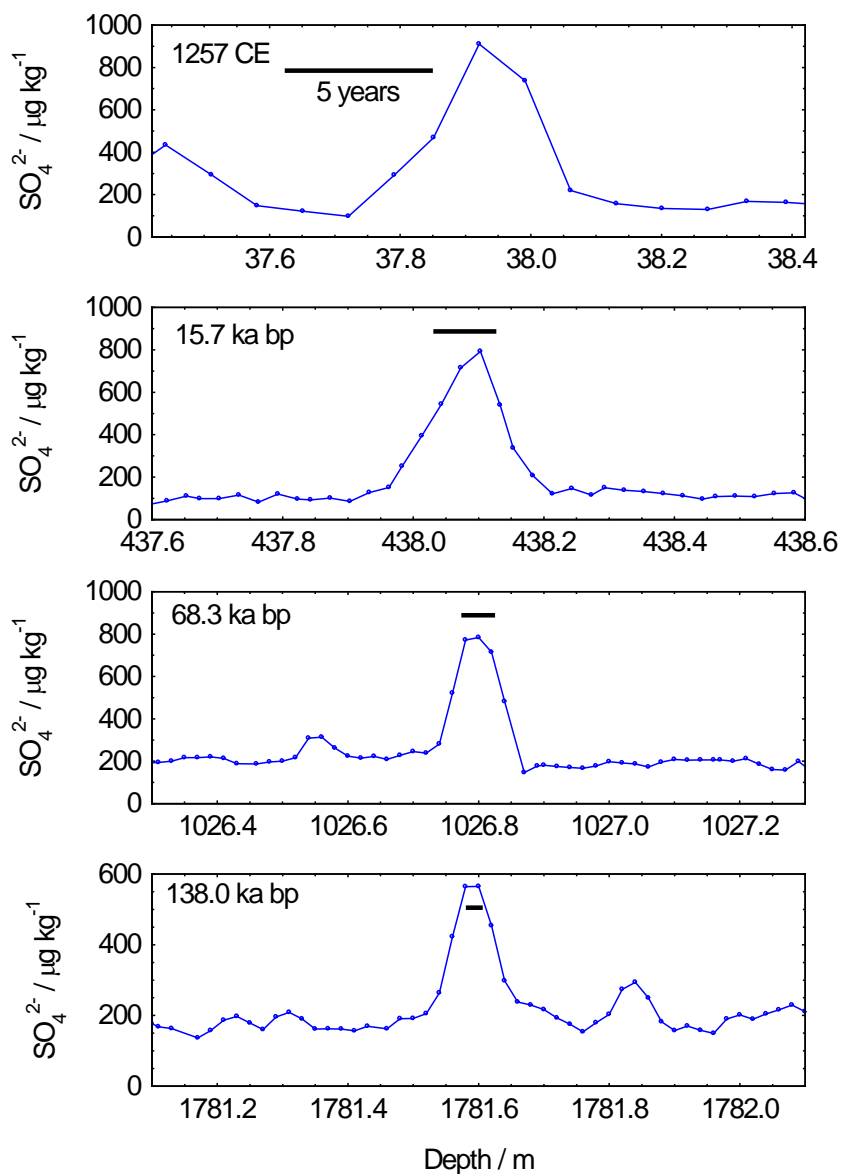


106

107

108 **Figure 1.** Comparison of FIC and IC data for two sections of the EDC ice core. In the section from 130 to 145 m, FIC peaks are consistently
109 lower than those of IC while in the section from 390 metres, the concentrations are essentially the same in the two methods.

110 Beyond 358.6 m, the data were used without correction. Volcanic peaks, standing clear of the sulfate background, remain
111 visible beyond 200 ka. It is clear that diffusion has occurred, making peaks considerably wider in years (and consequently
112 smaller in amplitude) than they were at the time of deposition; however, thinning seems to balance diffusion rather closely
113 (Fig. 2). The result is that peaks remain within about a 30 cm window at all depths to 200 ka, and the resolution of the data
114 remains adequate to estimate peak areas.



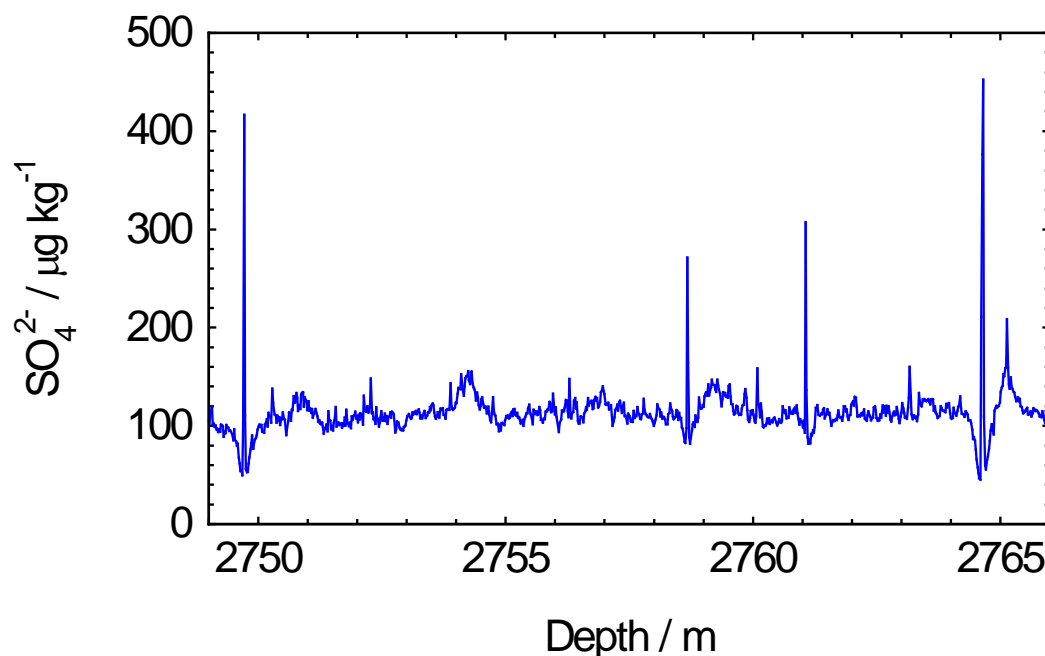
115

116 Figure 2. Examples of volcanic peaks at different depths and ages. The 1257 peak (top panel) is shown after application of the
117 correction described above. The black horizontal bar on each plot represents 5 years at each depth. Dots represent the mid-
118 depths of individual samples.

119 The dataset includes sections of missing data, where no FIC sulfate data are available. Mainly this consists of short sections at
120 the end of core lengths, but there are some longer sections where data were not taken either because of poor core quality or
121 instrument problems. Out of 2070 m of ice, there are 25 gaps longer than 30 cm, consisting in total of 19 m of ice. We discuss
122 our treatment of missing data under methods.



123 In deeper ice, it has been observed (Traversi et al., 2009) that anomalous spikes in sulfate concentration form through an as-
124 yet uncharacterised post-depositional process. In Fig. 3 we show clear examples of this artefact at about 400 ka; sulfate appears
125 to have been “sucked” from the surrounding background into a sharp peak. We observed signs of this behaviour as shallow as
126 2500 m (300 ka). To avoid any possibility of including such artefact peaks, we restrict our subsequent analysis to the past 200
127 kyr. This also avoids the problem that peaks become harder to distinguish from background with greater depth.



128

129 Figure 3. An example of four artefact peaks in ice aged just over 400 ka.

130 Material for the last few decades was not available in the EDC ice core because the top few metres were not retrieved. However,
131 the Pinatubo period has been studied previously at Dome C using snow pits (Castellano et al., 2005). The observed peak
132 (deposition of 10.7 mg m^{-2}) encompassed both Pinatubo and the eruption of Mount Hudson in Chile, which could not be
133 separated. However, the two eruptions have been resolved at South Pole (Cole-Dai and Mosley-Thompson, 1999), allowing
134 a fraction of deposition in the combined peak to be assigned to each eruption. Using the same fraction, we estimate 7.5 mg m^{-2}
135 for the Pinatubo sulfate deposition at Dome C, used later as part of benchmarking our data.

136 3. Methods

137 We applied the following method of calculating sulfate deposition. The ice core volcanic record consists of numerous sharp
138 spikes of sulfuric acid input, superimposed on a noisy background. The background consists mainly of sulfate from oxidation



139 of marine biogenic emissions of dimethylsulfide, with small contributions from sea salt as well as background volcanic sulfate.
140 Based on sulfate concentration measurements (Legrand and Delmas, 1984) and measurements of $\delta^{34}\text{S}$ in ice at South Pole
141 (Patris et al., 2000), the volcanic contribution to the background is estimated as less than 10%. In order to calculate the sulfate
142 deposition during each individual eruption event, we subtract the background and then sum the area across the peak, correcting
143 for ice thinning.

144 To correct for the background, we subtracted a running median from the dataset. The median is preferred to the mean because
145 the mean includes the volcanic peaks while the median should, if well-chosen, exclude the peaks. The time period over which
146 the median is calculated needs to be short enough that it follows the varying background but long enough that it will never use
147 the values within volcanic peaks. In our standard calculations we used 200 years, but other periods were also tested in
148 sensitivity studies. Varying the period over which the median was calculated between 100 and 400 years changed the total
149 number of peaks above a threshold of 20 mg m^{-2} by up to 10% compared to the standard case (200 years) but did not affect the
150 profile of peaks with time.

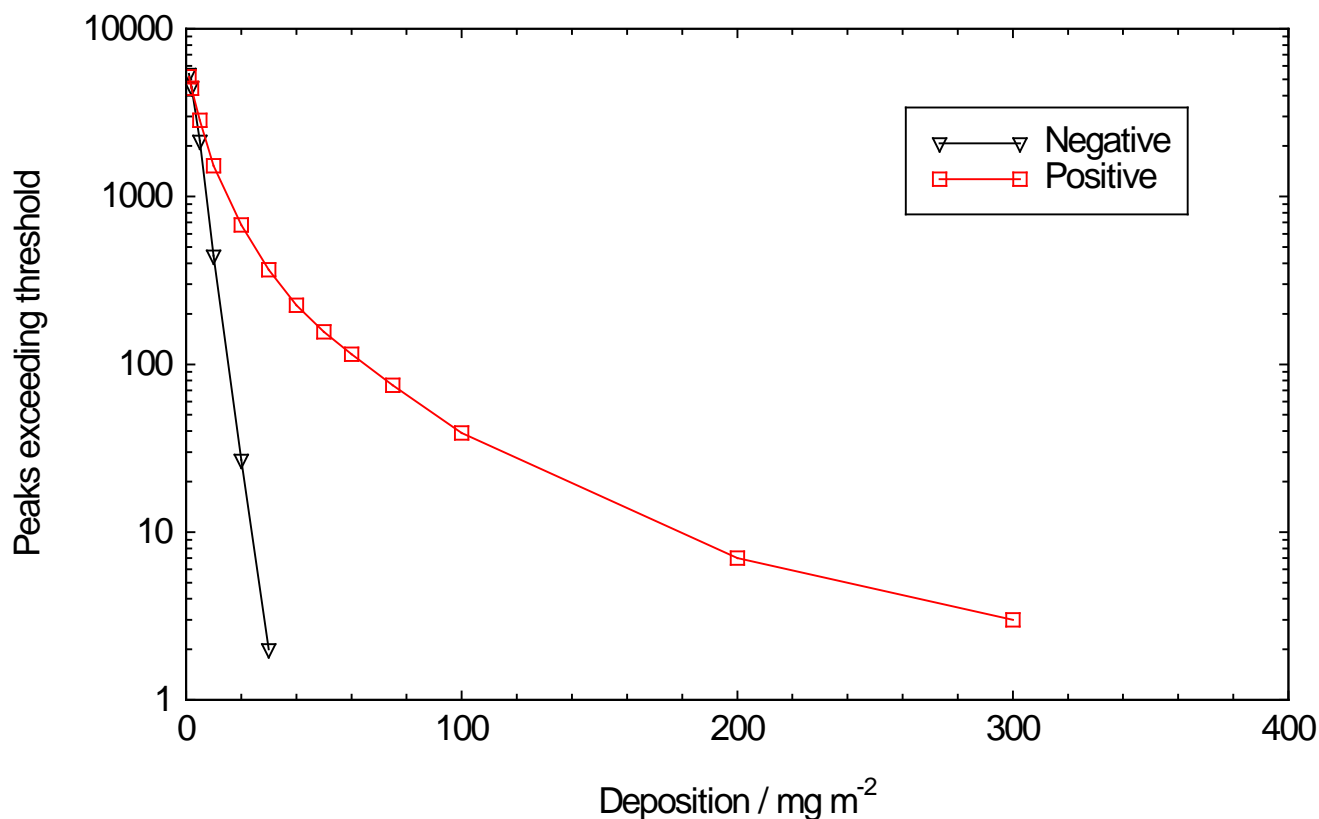
151 Having subtracted the background, we calculate the total amount of sulfate deposited to the snow per unit area across the whole
152 eruption. A key assumption is that the sulfate is mainly deposited by dry deposition, which is expected to be true at a site like
153 Dome C with its very low snow accumulation rate. This justifies the underlying assumption that the sulfate flux scales with
154 the amount of sulfate injected into the stratosphere. We first calculate the annual flux of sulfate in each sample ($\mu\text{g m}^{-2} \text{ a}^{-1}$) as
155 $F = C * A$, where C is the concentration in a slice of ice ($\mu\text{g kg}^{-1}$), and A is the snow accumulation rate ($\text{kg m}^{-2} \text{ a}^{-1}$). We then
156 calculate the total deposition in each sample ($\mu\text{g m}^{-2}$) by multiplying the flux by the time period represented in each sample;
157 this is done by using the accumulation rate and thinning parameter derived in the AICC2012 age model (Bazin et al., 2013) to
158 calculate the annual layer thickness. Finally, since the FIC data are effectively averages for discrete slices, we sum the
159 deposition (above background) in each of the samples that contribute to a particular peak to get the total deposition for an
160 individual eruption. This method automatically corrects the flux for the ice thinning (which is already 73% at the depth (2090
161 m) of 200 ka ice.

162 The algorithm we use searches for local maxima in the residual (after subtraction of the background) and calculates the sum
163 of samples across a chosen summing width across each maximum. The summing width needs to be large enough to include
164 all the volcanic sulfate after diffusion (Barnes et al., 2003). Visual observation suggests that a width of 30 cm (ie samples
165 within 15 cm of the concentration maximum) is appropriate at all depths between the surface and 2100 m. This width is justified
166 because diffusion more or less keeps pace with thinning at EDC. However, this width was also varied in sensitivity studies.
167 Varying the integration width between 20 and 40 cm altered the total number of peaks above a threshold of 20 mg m^{-2} by up
168 to 10% compared to the standard case (30 cm) but did not affect the profile of peaks with time. At many depths, an integration
169 width of 20 cm is clearly too narrow to capture the full peak, while 40 cm includes sections of background, so the uncertainty
170 induced by this parameter is below 10%.



171 Our method calculates numerous small peaks that are caused simply by variations around the background. To estimate this
172 variation we also calculate “negative” peaks around our median line. We then separately sum the number of peaks and negative
173 peaks in bins exceeding particular deposition fluxes (Figure 4). At a deposition of $10 \mu\text{g m}^{-2}$, there is still a substantial number
174 of negative peaks (441 in 200 kyr, compared to 1518 positive peaks). At 20 mg m^{-2} , there are very few negative peaks (28 in
175 200 kyr compared to 678 positive peaks), suggesting that 96% of peaks we count at this level are volcanic eruption peaks, and
176 supporting our choice of 20 mg m^{-2} as the background threshold for counting peaks. There are no negative peaks at 40 mg m^{-2} .
177 This indicates that, while we could investigate volcanoes with lower deposition fluxes in some time periods, we should
178 restrict ourselves to peaks above 20 mg m^{-2} in order to count peaks of similar size consistently over 200 kyr.

179 In our standard calculation we treated missing data as having the concentration of the background, i.e. those sections did not
180 contribute to the size of volcanic peaks in which they were embedded. We also did a calculation where we set the value of all
181 missing sections less than 30 cm thick to be the average of the adjacent samples: this increased the total count of peaks > 20
182 mg m^{-2} by only 11 (out of 678). It is likely that the longer sections of missing data (25 sections > 30 cm, totalling 19 m of ice)
183 would have contained some peaks but assuming they contain the same proportion of volcanoes as the measured parts we have
184 probably missed less than 10 peaks with deposition $> 20 \text{ mg m}^{-2}$.



185



186 Figure 4. Distribution of positive and negative peaks exceeding different deposition fluxes, summed over the past 200 kyr.
187 Sulfur isotopes were measured on discrete samples of ice cut at high resolution (every 2-3 cm) across 21 volcanic sulfate
188 events from Dome C between 10.1 and 96.1 ka. Samples were melted and measured for concentration by ion chromatography.
189 Based on the concentration, a volume corresponding to 20 nmol of sulfate was dried down and purified through anion exchange
190 columns following the method previously described (Burke et al., 2019). Each sample was measured at least twice for $\delta^{34}\text{S}$
191 and $\delta^{33}\text{S}$ by multi-collector inductively coupled plasma mass spectrometry, where

$$192 \delta^x\text{S} = \left(\frac{{}^x\text{S}/{}^{32}\text{S}}{\text{sample}} / \frac{{}^x\text{S}/{}^{32}\text{S}}{\text{reference}} \right) - 1$$

193 and x is either 33 or 34. Mass independent fractionation was calculated as

$$194 \Delta^{33}\text{S} = \delta^{33}\text{S} - ((\delta^{34}\text{S} + 1) * 0.515 - 1)$$

195 The uncertainty for these $\Delta^{33}\text{S}$ measurements is 0.14‰ (2 s.d.). Only sulfate that has been in the stratosphere shows a non-
196 zero signal of $\Delta^{33}\text{S}$, and so if the maximum magnitude $\Delta^{33}\text{S}$ across a peak is greater than 0.14‰, the eruption is considered
197 stratospheric.

198 4. The frequency of eruptions recorded in Antarctica

199 A few of the most recent sulfate layers can be correlated to specific eruptions allowing some calibration of the record to the
200 magnitude of explosive eruptions (Gao et al., 2008; Sigl et al., 2015), but most layers cannot be linked to a source. As a
201 benchmark Table 1 lists four sulfate peaks in Dome C where the eruption location and magnitude are also known, including
202 the 1991 Pinatubo eruptions (Castellano et al., 2005). The benchmark data (all from tropical eruptions) imply that peaks above
203 our chosen threshold of 20 mg m⁻² are likely to be M>6.5 eruptions.

Eruption	Dome C deposition (mg m ⁻²)	Magnitude	Emission (Tg SO ₂)
Pinatubo 1991	7.5	6.1	18
Krakatoa 1883	13.2	6.4	19
Rinjani/Samalas 1257	74.5	7.0	119
Tambora 1815	53	7.0	56

204

205 Table 1. Identified sulfate peaks in Dome C with magnitude and estimated emission (Toohey and Sigl, 2017).

206 Various attempts have been made to derive SO₂ emissions (in Mt or Tg of S or SO₂) from ice core deposition (in mg m⁻² of
207 sulfate) (Sigl et al., 2022). However this is difficult when there is only one ice core location, and the location of the eruption
208 is unknown. Model studies show that the ratio of deposition in Antarctica to emissions depends on latitude of eruption, the
209 height the plume reaches, and the time of year of the eruption (Marshall et al., 2021). As a rough estimate using emissions
210 values calculated in the literature (Toohey and Sigl, 2017) we can deduce that for tropical eruptions, SO₂ emissions in Tg SO₂

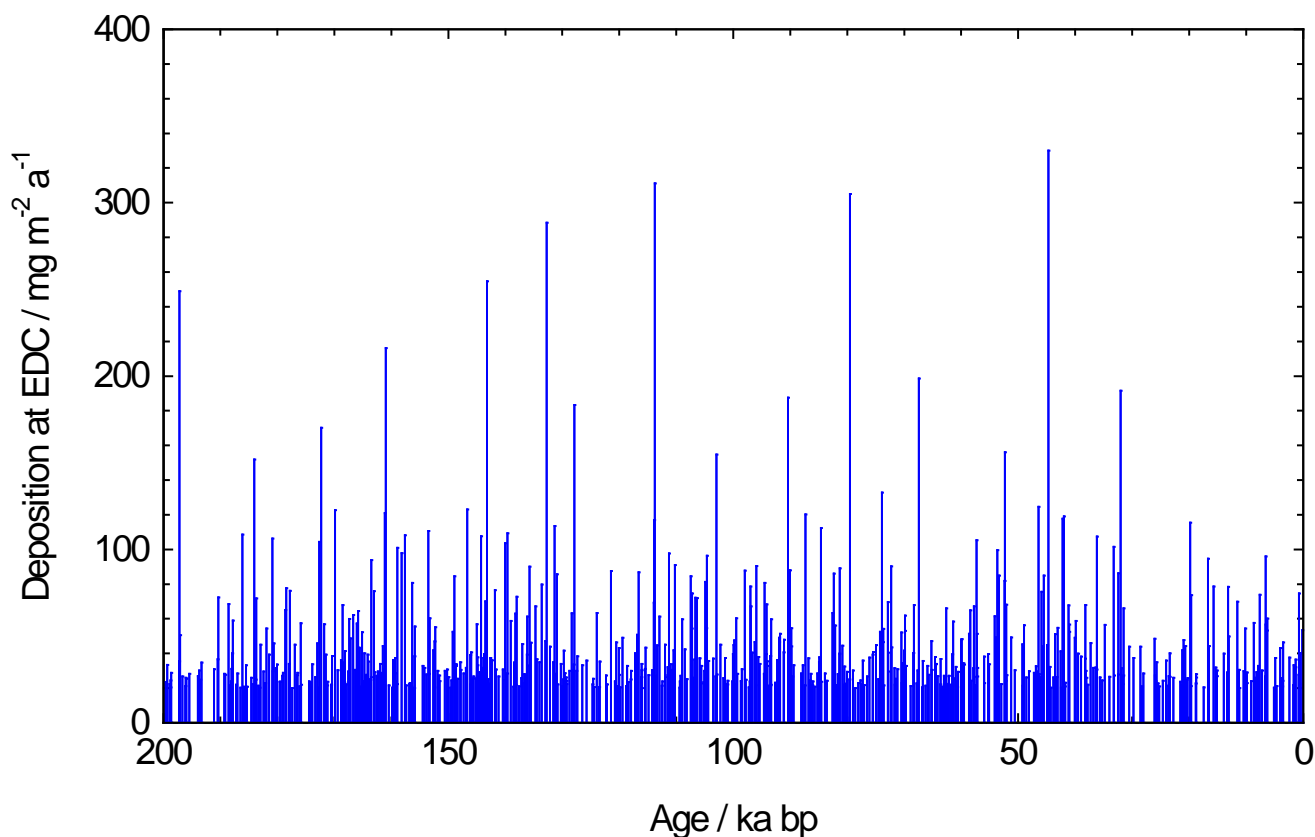


211 are about 1-2 times higher than our measured EDC depositions in mg m^{-2} (Table 1). However the factor should certainly be
212 increased if eruptions occurred at high northern latitudes (Marshall et al., 2021).

213 Using our base set of parameters (200 year median calculation, 30 cm summation of layers per volcano, missing values treated
214 as having background concentration), we find that the last 200 kyr contains 678 volcanic events with deposition rates greater
215 than 20 mg m^{-2} (Fig. 4); this gives an average of 3.4 per millennium. Although our method is identical in concept, we calculate
216 rather more peaks greater than 20 mg m^{-2} (2.87/ka vs 2.21/kyr) for the period 9-60 ka than that estimated for EDC by previous
217 work (Lin et al., 2022). This difference seems to arise because our method calculates higher integrals for smaller peaks,
218 suggesting that the difference is related to the way that the background is calculated and/or the way that we deal with the width
219 of each peak. This is supported by the fact that at the extreme of our parameter choices (20 cm peak widths, and 100 year
220 interval for calculating the median background) our estimates converge with those of the previous work (Lin et al., 2022).
221 There are only 76 peaks with fluxes larger than that of Rinjani/Samalas (1257), making this a 1 in 2500 year event. A time
222 series of all eruptions greater than 20 mg m^{-2} is shown in Fig. 5.

223 Our results are also consistent with independent estimates of the global magnitude-frequency relationship (Rougier et al.,
224 2018). Based on data shown in Table 4, sulfate peaks $> 20 \text{ mg m}^{-2}$ should have magnitudes ≥ 6.5 while sulfate peaks $> 50 \text{ mg}$
225 m^{-2} should have magnitudes ≥ 7 . The analysis of global terrestrial data (Rougier et al., 2018) gives an estimate of $M \geq 6.5$
226 eruptions as 2.75/kyr (confidence interval (CI) 1.6-4.3) and an estimate of $M \geq 7$ eruptions as 0.8/kyr (CI 0.48 to 1.47). Thus
227 the event rates based on sulfate events at $> 20 \text{ mg m}^{-2}$ (3.4/kyr) and $> 50 \text{ mg m}^{-2}$ (0.78/kyr) are well within the uncertainty
228 ranges of the estimates from the global terrestrial record.

229 The largest peaks in the past 200 kyr deposited around 300 mg m^{-2} . The largest recorded eruption in the timeframe that could
230 accommodate the Toba eruption (Crick et al., 2021; Svensson et al., 2013) has a flux of 133 mg m^{-2} (16th largest in our record),
231 Thus it unlikely that, in terms of global dispersion of sulfate aerosol, Toba was the most significant volcanic climate forcing
232 event of the past 200 kyr.

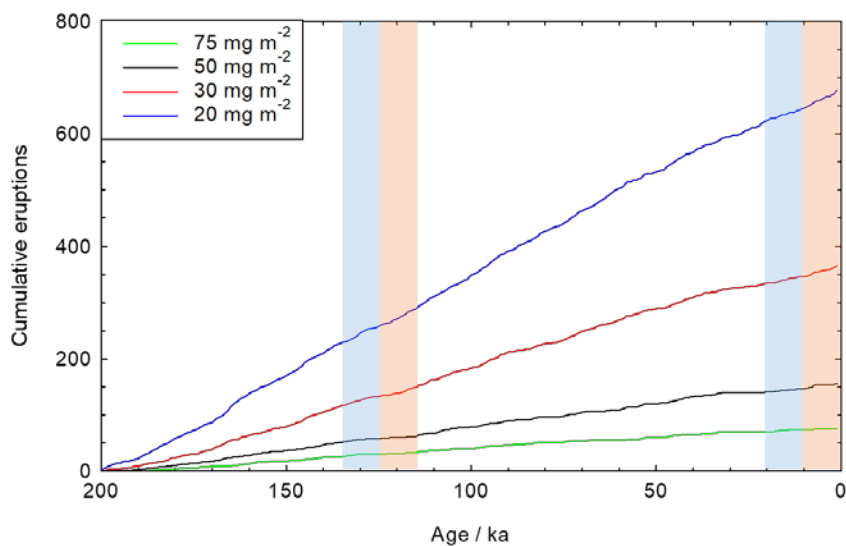


233

234 Figure 5. The deposition flux of sulfate for events with deposition more than 20 mg m^{-2} over the last 200 kyr.

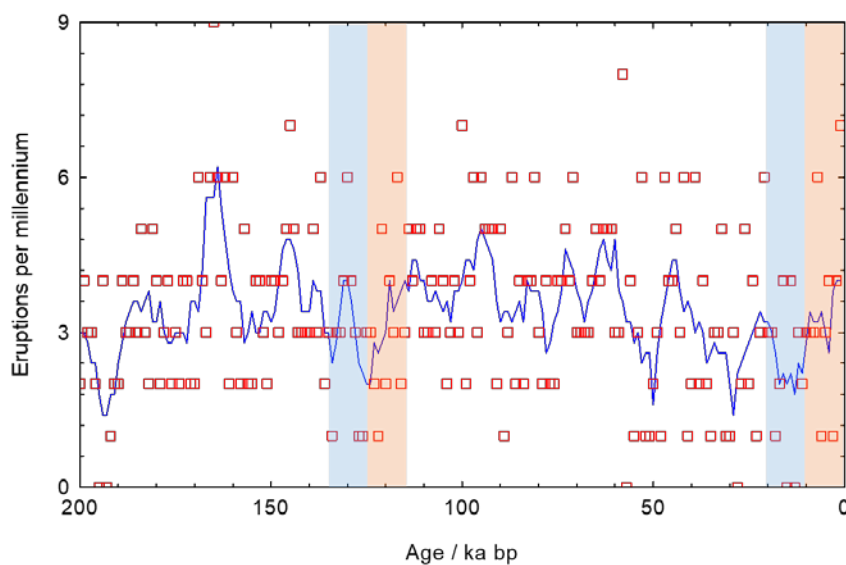
235 To assess whether there are particular periods with high or low numbers of eruptions, we plot the cumulative number of large
236 sulfate deposition events with time (Figure 6). Concentrating mainly on the result for eruptions greater than 20 mg m^{-2} because
237 of the greater numbers involved, the trend is linear, indicating a steady state of large explosive eruptions across two glacial
238 cycles. There is no sign of an increased slope (i.e., increased eruption frequency) at the two periods of deglaciation or
239 interglacials. This can be seen in Fig. 7. The number of eruptions per millennium is very variable, as is to be expected from
240 counting statistics for such small numbers. As a result the time series plot of the occurrence data is very scattered (Fig. 7).
241 Nonetheless it is quite obvious that, at Dome C, both periods of deglaciation tend to have eruption frequencies at the lower
242 end of the range, rather than increased rates.

243



244

245 Figure 6: Cumulative eruption numbers over the past 200 kyr recorded in the Dome C ice core for different eruption deposition fluxes of
246 sulfate. Periods of deglaciation marked with blue bar, interglacials with orange bar.



247

248 Figure 7: Eruption numbers per millennium (red) and 5 kyr running mean (blue). Periods of deglaciation marked with blue
249 bar, interglacials with orange bar.

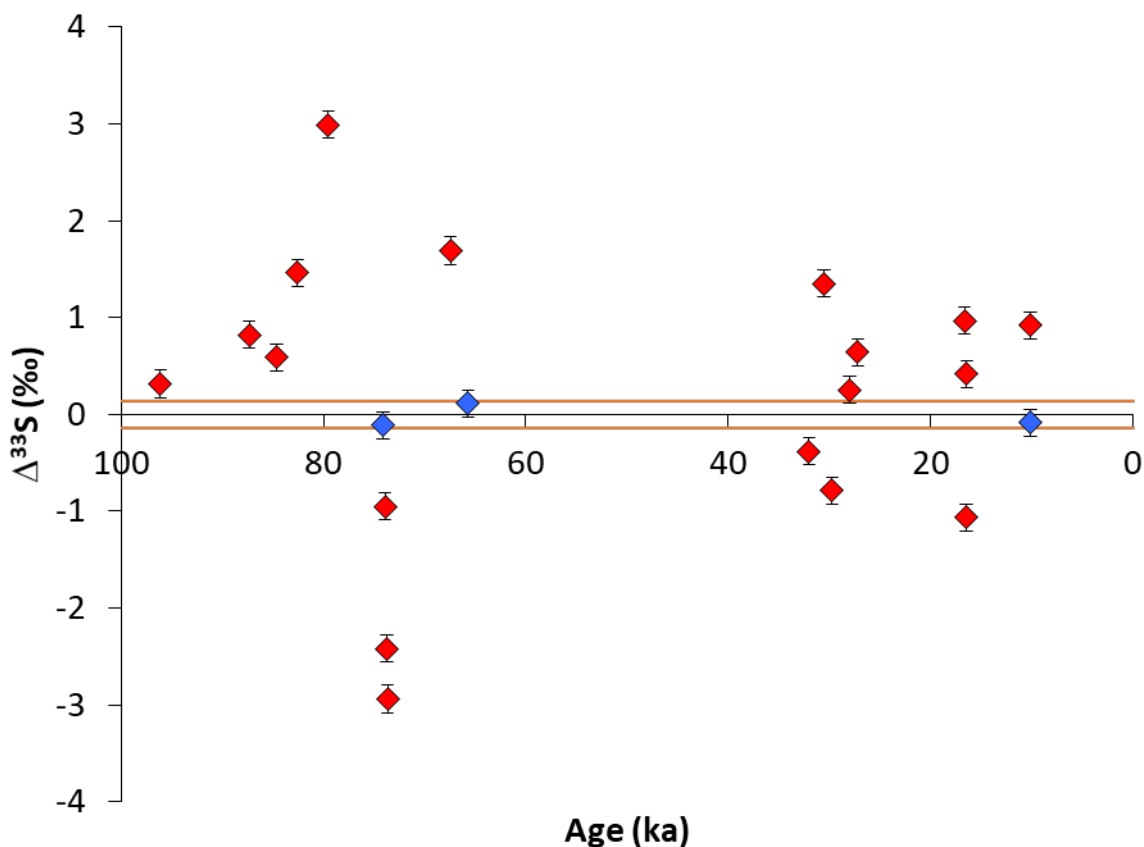
250 We explored other ways of analysing the ice core data to assess whether a climate cycle signal can be recognised. Using
251 spectral analysis on the millennial eruption counts, we identified a possible peak corresponding to a 20 kyr period (frequency
252 similar to precession) that emerges with weak statistical significance. This certainly needs to be confirmed in other records.



253 Although there have been weak indications of a 23 kyr period in Mediterranean tephra data (Kutterolf et al., 2019) it is difficult
254 to envisage a mechanism by which precession would influence global volcanism, given that it leads to much weaker changes
255 in ice sheet unloading and sea level compared to the longer (of order 100 kyr) period. Temperature and snow accumulation
256 rate at the EDC site show only very weak precessional power (Jouzel et al., 2007), so precessional changes in deposition
257 efficiency are unlikely to be strong. However, precession significantly influences tropical hydroclimate and the position and
258 width of the ITCZ (Singarayer et al., 2017). These changes could affect the washout of aerosol from eruptions in tropical
259 regions, and hence their ability to reach the stratosphere. There will certainly also be an associated effect on the efficiency of
260 the Brewer Dobson circulation that transports aerosol to the poles through the stratosphere, although we are not aware of model
261 simulations of this transport involving significant changes in precession (Fu et al., 2020). Thus, if the 20 kyr period is confirmed
262 it might be ascribed to a small change in the effectiveness of transporting tropical or Northern Hemisphere eruption material
263 to Antarctica. We emphasise that there is no significant signal at the lower Milankovitch frequency corresponding to 40 kyr.
264 Our record is too short to make a meaningful assessment in frequency space of the ~100 kyr cycle on which deglaciations
265 occur, but we again emphasise that, if anything, we see lower numbers of recorded events across the two deglaciations.

266 5. Discussion

267 As described earlier, there are several challenges when interpreting this dataset as a record of global volcanism. First, there is
268 the difficulty of separating local tropospheric from larger magnitude stratospheric eruptions. Mass-independent sulfur isotopes
269 in ice cores can be used to determine whether a volcanic event was stratospheric (Baroni et al., 2008; Burke et al., 2019;
270 Gautier et al., 2019; Savarino et al., 2003b). Isotope analysis of large sulfate peaks from the last 2600 years at Dome C (Gautier
271 et al., 2019) indicates 11 tropospheric and 49 stratospheric events, with 4 events showing an inconclusive signal. All the
272 largest events ($>20 \text{ mg m}^{-2}$ deposited at Dome C) were stratospheric. In this study, we tested if the proportion of stratospheric
273 events recorded at Dome C was the same earlier in the record by measuring an additional 21 events from Dome C between
274 10.1 and 96.1 ka following previous methods (Burke et al., 2019). We found (Fig. 8 and supplementary table) that most (18
275 out of 21; 15 out of 17 for deposition $>20 \text{ mg m}^{-2}$) volcanic signals in Dome C are stratospheric, consistent with its isolated
276 location away from most volcanic sources. The sulfur isotope data therefore show that more than 80% of the volcanic events
277 recorded at Dome C involved stratospheric input due to large explosive eruptions.



278

279 Fig. 8. Values of $\Delta^{33}\text{S}$ for 21 large volcanic eruptions recorded at Dome C in the last 100 kyr. Values outside a range of $\pm 0.14\%$
280 are considered to indicate a stratospheric eruption.

281 Second, sulfate peak amplitudes can vary strongly between core sites that are close together, and major peaks can even be
282 missing at a single site (Gautier et al., 2016; Wolff et al., 2005). This problem is particularly pronounced at sites with low
283 snow accumulation where years may be missing, like Dome C (Wolff et al., 2005), but these sites must be used to investigate
284 long records of volcanism. This issue will cause variability in measured eruption rates which should average out over longer
285 time periods.

286 Third, there will be a significant bias in the record of global explosive volcanism in Antarctica as a consequence of source
287 locations and magnitude. Northern Hemisphere extratropical eruptions ($>23^\circ\text{N}$) will be under-represented and biased towards
288 very large eruptions with the likelihood of sulfate aerosol moving into the Southern Hemisphere being a function of source
289 latitude and magnitude (Marshall et al., 2021). Thus the Antarctic volcanic record will be biased by larger depositional fluxes
290 for tropical and especially Southern Hemisphere extratropical sources while exhibiting smaller depositional fluxes or even
291 missing events for Northern Hemisphere extratropical eruptions.



292 The bias in source locations with extratropical Northern Hemisphere eruptions being underrepresented may result in net under-
293 recording. The estimates of Sigl et al. (Sigl et al., 2015) suggest that around 80% of eruptions giving the greatest global aerosol
294 loadings are recorded in Antarctica. Our Antarctic ice core data therefore might underestimate the number of eruptions in each
295 size class by perhaps 20%, somewhat compensated by the ~20% of eruptions from regional volcanoes recorded in Antarctica
296 that are tropospheric (Gautier et al., 2019). To first order, both the over-recording due to tropospheric eruptions and the under-
297 recording of extratropical northern hemisphere eruptions should operate in a similar way through time (excluding any effects
298 of changing transport strength discussed above) and across a range of eruption magnitudes. Thus the shape of the plots of
299 number of eruptions versus time and of number against sulfur deposition should be unaffected.

300 Finally the ice core record in Antarctica is a record of large silicic explosive eruptions (likely mostly $M > 6.5$). A spatial
301 analysis of the LaMEVE database of Quaternary explosive eruptions (Fig. 1 in Brown et al., 2014) show that the sources of
302 these big eruptions are largely in low and mid latitudes. This spatial bias is a consequence of present day plate boundary
303 distributions. Tectonic settings conducive to forming large silicic magma reservoirs and characterised by caldera forming large
304 magnitude explosive eruptions are typically in low and mid latitudes where deglaciation effects on melt generation are likely
305 to be absent or greatly reduced. There are no known $M > 7$ Quaternary eruption from a northern high latitude volcano ($>60^\circ\text{N}$)
306 (Brown et al., 2014). Thus our findings are not necessarily in contradiction to previous findings (such as Huybers and
307 Langmuir, 2009) because the Antarctic record is biased towards silicic explosive eruption in the southern hemisphere and
308 tropical regions.

309 **6. Conclusions**

310 In this study we have extended the study of explosive eruptions recorded at the EDC ice core to 200 ka BP, using a method
311 that should consistently record large volcanic events through time. The record mainly represents large magnitude explosive
312 eruptions with magnitudes of 6.5 or above. We find no systematic variability through time, though there could be a small effect
313 of transport efficiency manifested in an apparent 20 kyr period that needs to be confirmed in other cores. There is no sign of
314 any increase in eruption frequency at deglaciations. This does not of course negate the likelihood that unloading of ice did
315 cause increased frequencies in regions susceptible to such effects, such as Iceland. However, taking into account the S isotope
316 evidence that most large eruptions recorded at EDC are stratospheric, our record is probably representative for the major events
317 influencing climate through stratospheric sulfate. We cannot rule out an effect from volcanism on the balance of CO_2
318 production and removal at deglaciation (Huybers and Langmuir, 2009), but it would have to operate only through smaller high
319 latitude eruptions and/or submarine volcanism. Finally we comment that it is difficult to study volcanism in ice cores over a
320 period longer than 200 ka until the post-depositional effects leading to artefact peaks are better understood.

321 **Data availability**



322 The sulfate data on which this paper is based are available at the NCEI paleoclimate data center, at
323 <https://www.ncdc.noaa.gov/paleo-search/study/31332>; the depths and ages of large volcanic peaks in the EDC ice core that
324 form the basis for Figures 5-7 are listed at Wolff, Eric W; Severi, Mirko (2021): Fluxes of largest volcanic peaks in the EDC
325 sulfate record. PANGAEA, <https://doi.org/10.1594/PANGAEA.926087>

326 The age model data, including accumulation rate and thinning factor, is available in the supplement to the Bazin et al. (2013)
327 and in the Pangaea database at <https://doi.org/10.1594/PANGAEA.824865>

328 The code used to identify, sum and count peaks, as well as the input data file, is attached as a supplement to this paper.

329 **Author contribution**

330 EW, AB and RSJS conceived the idea for this paper. MS provided the sulfate data that were analysed by the Firenze laboratory.
331 EW and SHM studied the ice core data to determine which samples should undergo S isotope analysis. SHM, EAD and LC
332 prepared the samples for S isotope analysis, while AB, HMI and LC carried out those analyses. EWW developed and
333 implemented the sulfate peak identification method, analysed and sensitivity tested the data. AB and JWBR investigated the
334 spectral properties of the data. RSJS and SHM advised about the nature of the volcanic record, including marine and terrestrial
335 data. RSJS, EWW and AB prepared sections of text and all authors edited the text.

336 **Competing interests**

337 One of the authors is a member of the CP editorial board. The authors declare that they have no other conflicts of interest.

338 **Acknowledgments**

339 This project has been supported by the Leverhulme Trust (RPG-2015-246), by a Royal Society Professorship to EWW, and
340 by a Marie Curie Career Integration Grant to AB. This work is a contribution to the European Project for Ice Coring in
341 Antarctica (EPICA), a joint European Science Foundation/European Commission (EC) scientific programme, funded by the
342 EU and by national contributions from Belgium, Denmark, France, Germany, Italy, The Netherlands, Norway, Sweden,
343 Switzerland and the UK. The main logistic support at Dome C was provided by IPEV and PNRA. We thank Michael Sigl for
344 help with data on estimated emissions of SO₂.

345 **Financial support**

346 This research has been supported by the Leverhulme Trust (grant RPG-2015-246), by a Royal Society Professorship (grant no.
347 RP/R/180003), and by a Marie Curie Career Integration Grant (CIG14-631752).

348 **Figure captions**

349 Figure 1. Comparison of FIC and IC data for two sections of the EDC ice core. In the section from 130 to 150 m, FIC peaks are consistently
350 lower than those of IC while in the section from 390 metres, the concentrations are the same in the two methods.



351 Figure 2. Examples of volcanic peaks at different depths and ages. The 1257 peak (top panel) is shown after application of the
352 correction described above. The black horizontal bar on each plot represents 5 years at each depth. Dots represent the mid-
353 depths of individual samples.

354 Figure 3. An example of four artefact peaks in ice aged just over 400 ka.

355 Figure 4. Distribution of positive and negative peaks exceeding different deposition fluxes, summed over the past 200 kyr.

356 Figure 5. The deposition flux of sulfate for events with deposition more than 20 mg m⁻² over the last 200 kyr.

357 Figure 6: Cumulative eruption numbers over the past 200 kyr recorded in the Dome C ice core for different eruption deposition
358 fluxes of sulfate. Periods of deglaciation marked with blue bar, interglacials with orange bar.

359 Figure 7: Eruption numbers per millennium (red) and 5 kyr running mean (blue). Periods of deglaciation marked with blue
360 bar, interglacials with orange bar.

361 Fig. 8. Values of $\Delta^{33}\text{S}$ for 21 large volcanic eruptions recorded at Dome C in the last 100 kyr. Values outside a range of $\pm 0.14\%$
362 are considered to indicate a stratospheric eruption.

363

364 References

365

366 Barnes, P. R. F., Wolff, E. W., Mader, H. M., Udisti, R., Castellano, E., and Rothlisberger, R.: Evolution of chemical peak shapes in the
367 Dome C, Antarctica, ice core, *J. Geophys. Res.*, 108, doi:10.1029/2002JD002538, 2003.

368

369 Baroni, M., Savarino, J., Cole-Dai, J. H., Rai, V. K., and Thiemens, M. H.: Anomalous sulfur isotope compositions of volcanic sulfate over
370 the last millennium in Antarctic ice cores, *J. Geophys. Res.-Atmos.*, 113, doi: 10.1029/2008jd010185, 2008.

371

372 Bazin, L., Landais, A., Lemieux-Dudon, B., Kele, H. T. M., Veres, D., Parrenin, F., Martinerie, P., Ritz, C., Capron, E., Lipenkov, V.,
373 Loutre, M. F., Raynaud, D., Vinther, B., Svensson, A., Rasmussen, S. O., Severi, M., Blunier, T., Leuenberger, M., Fischer, H., Masson-
374 Delmotte, V., Chappellaz, J., and Wolff, E. W.: An optimised multi-proxy, multi-site Antarctic ice and gas orbital chronology (AICC2012):
375 120-800 ka, *Climate of the Past* 9, 1715-1731, 2013.

376

377 Brown, S. K., Croswell, H. S., Sparks, R. S. J., Cottrell, E., Deligne, N. I., Guerrero, N. O., Hobbs, L., Kiyosugi, K., Loughlin, S. C.,
378 Siebert, L., and Takarada, S.: Characterisation of the Quaternary eruption record: analysis of the Large Magnitude Explosive Volcanic
379 Eruptions (LaMEVE) database, *Journal of Applied Volcanology*, 3, 5, doi: 10.1186/2191-5040-3-5, 2014.

380

381 Burke, A., Moore, K. A., Sigl, M., Nita, D. C., McConnell, J. R., and Adkins, J. F.: Stratospheric eruptions from tropical and extra-tropical
382 volcanoes constrained using high-resolution sulfur isotopes in ice cores, *Earth planet. Sci. Lett.*, 521, 113-119, doi:
383 <https://doi.org/10.1016/j.epsl.2019.06.006>, 2019.

384

385 Castellano, E., Becagli, S., Hansson, M., Hutterli, M., Petit, J. R., Rampino, M. R., Severi, M., Steffensen, J. P., Traversi, R., and Udisti, R.:
386 Holocene volcanic history as recorded in the sulfate stratigraphy of the European Project for Ice Coring in Antarctica Dome C (EDC96) ice
387 core, *J. Geophys. Res.*, 110, D06114, doi:06110.01029/02004JD005259, 2005.

388

389 Castellano, E., Becagli, S., Jouzel, J., Migliori, A., Severi, M., Steffensen, J. P., Traversi, R., and Udisti, R.: Volcanic eruption frequency
390 over the last 45 ky as recorded in Epica-Dome C ice core (East Antarctica) and its relationship with climatic changes, *Global and Planetary
391 Change*, 42, 195-205, 2004.

392



- 393 Cole-Dai, J., Ferris, D. G., Kennedy, J. A., Sigl, M., McConnell, J. R., Fudge, T. J., Geng, L., Maselli, O. J., Taylor, K. C., and Souney, J.
394 M.: Comprehensive Record of Volcanic Eruptions in the Holocene (11,000 years) From the WAIS Divide, Antarctica Ice Core, *Journal of*
395 *Geophysical Research: Atmospheres*, 126, e2020JD032855, doi: <https://doi.org/10.1029/2020JD032855>, 2021.
- 396
397 Cole-Dai, J. and Mosley-Thompson, E.: The Pinatubo eruption in South Pole snow and its potential value to ice-core paleovolcanis records,
398 *Ann. Glaciol.*, 29, 99-105, 1999.
- 399
400 Crick, L., Burke, A., Hutchison, W., Kohno, M., Moore, K. A., Savarino, J., Doyle, E. A., Mahony, S., Kipfstuhl, S., Rae, J. W. B., Steele,
401 R. C. J., Sparks, R. S. J., and Wolff, E. W.: New insights into the ~74ka Toba eruption from sulfur isotopes of polar ice cores, *Clim. Past*,
402 17, 2119-2137, doi: 10.5194/cp-17-2119-2021, 2021.
- 403
404 Fu, Q., White, R. H., Wang, M., Alexander, B., Solomon, S., Gettelman, A., Battisti, D. S., and Lin, P.: The Brewer-Dobson Circulation
405 During the Last Glacial Maximum, *Geophys. Res. Lett.*, 47, e2019GL086271, doi: <https://doi.org/10.1029/2019GL086271>, 2020.
- 406
407 Fujita, S., Parrenin, F., Severi, M., Motoyama, H., and Wolff, E. W.: Volcanic synchronization of Dome Fuji and Dome C Antarctic deep
408 ice cores over the past 216 kyr, *Clim. Past*, 11, 1395-1416, doi: 10.5194/cp-11-1395-2015, 2015.
- 409
410 Gao, C., Robock, A., and Ammann, C.: Volcanic forcing of climate over the past 1500 years: An improved ice core-based index for climate
411 models, *J. Geophys. Res.*, 113, D23111, 2008.
- 412
413 Gautier, E., Savarino, J., Erbland, J., Lanciki, A., and Possenti, P.: Variability of sulfate signal in ice core records based on five replicate
414 cores, *Climate of the Past*, 12, 103-113, doi: 10.5194/cp-12-103-2016, 2016.
- 415
416 Gautier, E., Savarino, J., Hoek, J., Erbland, J., Caillon, N., Hattori, S., Yoshida, N., Albalat, E., Albarede, F., and Farquhar, J.: 2600-years
417 of stratospheric volcanism through sulfate isotopes, *Nature Communications*, 10, 466, doi: 10.1038/s41467-019-08357-0, 2019.
- 418
419 Huybers, P. and Langmuir, C.: Feedback between deglaciation, volcanism, and atmospheric CO₂, *Earth planet. Sci. Lett.*, 286, 479-491, doi:
420 10.1016/j.epsl.2009.07.014, 2009.
- 421
422 Jouzel, J., Masson-Delmotte, V., Cattani, O., Dreyfus, G., Falourd, S., Hoffmann, G., Nouet, J., Barnola, J. M., Chappellaz, J., Fischer, H.,
423 Gallet, J. C., Johnsen, S., Leuenberger, M., Loulergue, L., Luethi, D., Oerter, H., Parrenin, F., Raisbeck, G., Raynaud, D., Schwander, J.,
424 Spahni, R., Souchez, R., Selmo, E., Schilt, A., Steffensen, J. P., Stenni, B., Stauffer, B., Stocker, T., Tison, J.-L., Werner, M., and Wolff, E.
425 W.: Orbital and millennial Antarctic climate variability over the last 800 000 years, *Science*, 317, 793-796, doi: 10.1126/science.1141038,
426 2007.
- 427
428 Jull, M. and McKenzie, D.: The effect of deglaciation on mantle melting beneath Iceland, *J. Geophys. Res.-Solid Earth*, 101, 21815-21828,
429 doi: 10.1029/96jb01308, 1996.
- 430
431 Kutterolf, S., Schindlbeck, J. C., Jegen, M., Freundt, A., and Straub, S. M.: Milankovitch frequencies in tephra records at volcanic arcs: The
432 relation of kyr-scale cyclic variations in volcanism to global climate changes, *Quat. Sci. Rev.*, 204, 1-16, doi:
433 10.1016/j.quascirev.2018.11.004, 2019.
- 434
435 Legrand, M. and Delmas, R. J.: The ionic balance of Antarctic snow: a 10-year detailed record, *Atmos. Environ.*, 18, 1867-1874, doi:
436 10.1016/0004-6981(84)90363-9, 1984.
- 437
438 Lin, J., Svensson, A., Hvidberg, C. S., Lohmann, J., Kristiansen, S., Dahl-Jensen, D., Steffensen, J. P., Rasmussen, S. O., Cook, E., Kjær,
439 H. A., Vinther, B. M., Fischer, H., Stocker, T., Sigl, M., Bigler, M., Severi, M., Traversi, R., and Mulvaney, R.: Magnitude, frequency and
440 climate forcing of global volcanism during the last glacial period as seen in Greenland and Antarctic ice cores (60–9 ka), *Clim. Past*, 18,
441 485-506, doi: 10.5194/cp-18-485-2022, 2022.
- 442
443 Littot, G. C., Mulvaney, R., Rothlisberger, R., Udisti, R., Wolff, E. W., Castellano, E., de Angelis, M., Hansson, M., Sommer, S., and
444 Steffensen, J. P.: Comparison of analytical methods used for measuring major ions in the EPICA Dome C (Antarctica) ice core, *Ann. Glaciol.*,
445 35, 299-305, 2002.
- 446
447 Mahony, S. H., Barnard, N. H., Sparks, R. S. J., and Rougier, J. C.: VOLCORE, a global database of visible tephra layers sampled by ocean
448 drilling, *Scientific Data*, 7, doi: 10.1038/s41597-020-00673-1, 2020.



- 449
450 Marshall, L. R., Schmidt, A., Johnson, J. S., Mann, G. W., Lee, L. A., Rigby, R., and Carslaw, K. S.: Unknown Eruption Source Parameters
451 Cause Large Uncertainty in Historical Volcanic Radiative Forcing Reconstructions, *Journal of Geophysical Research: Atmospheres*, 126,
452 e2020JD033578, doi: <https://doi.org/10.1029/2020JD033578>, 2021.
453
454 McConnell, J. R., Burke, A., Dunbar, N. W., Köhler, P., Thomas, J. L., Arienzo, M. M., Chellman, N. J., Maselli, O. J., Sigl, M., Adkins, J.
455 F., Bagenstos, D., Burkhardt, J. F., Brook, E. J., Buizert, C., Cole-Dai, J., Fudge, T. J., Knorr, G., Graf, H.-F., Grieman, M. M., Iverson, N.,
456 McGwire, K. C., Mulvaney, R., Paris, G., Rhodes, R. H., Saltzman, E. S., Severinghaus, J. P., Steffensen, J. P., Taylor, K. C., and Winckler,
457 G.: Synchronous volcanic eruptions and abrupt climate change ~17.7 ka plausibly linked by stratospheric ozone depletion, *Proceedings of*
458 *the National Academy of Sciences*, 114, 10035-10040, doi: 10.1073/pnas.1705595114, 2017.
459
460 Parrenin, F., Petit, J.-R., Masson-Delmotte, V., Basile, I., Jouzel, J., Lipenkov, V., Rasmussen, S., Schwander, J., Severi, M., Udisti, R.,
461 Veres, D., Vinther, B., and Wolff, E. W.: Volcanic synchronisation between the EPICA Dome C and Vostok ice cores
462 (Antarctica) 0-145 kyr BP, *Climate of the Past* 8, 1031-1045, 2012.
463
464 Patris, N., Delmas, R. J., and Jouzel, J.: Isotopic signatures of sulfur in shallow Antarctic ice cores, *J. Geophys. Res.-Atmos.*, 105, 7071-
465 7078, 2000.
466
467 Robock, A.: Volcanic eruptions and climate, *Rev. Geophys.*, 38, 191-219, doi: doi:10.1029/1998RG000054, 2000.
468
469 Rougier, J., Sparks, R. S. J., Cashman, K. V., and Brown, S. K.: The global magnitude–frequency relationship for large explosive volcanic
470 eruptions, *Earth planet. Sci. Lett.*, 482, 621-629, doi: <https://doi.org/10.1016/j.epsl.2017.11.015>, 2018.
471
472 Ruth, U., Barnola, J. M., Beer, J., Bigler, M., Blunier, T., Castellano, E., Fischer, H., Fundel, F., Huybrechts, P., Kaufmann, P., Kipfstuhl,
473 J., Lambrecht, A., Morganti, A., Oerter, H., Parrenin, F., Rybak, O., Severi, M., Udisti, R., Wilhelms, F., and Wolff, E. W.: "EDML1": A
474 chronology for the EPICA deep ice core from Dronning Maud Land, Antarctica, over the last 150,000 years, *Climate of the Past*, 3, 475-
475 484, 2007.
476
477 Savarino, J., Bekki, S., Cole-Dai, J. H., and Thiemens, M. H.: Evidence from sulfate mass independent oxygen isotopic compositions of
478 dramatic changes in atmospheric oxidation following massive volcanic eruptions, *J. Geophys. Res.*, 108, 4671, 2003a.
479
480 Savarino, J., Romero, A., Cole-Dai, J., Bekki, S., and Thiemens, M. H.: UV induced mass-independent sulfur isotope fractionation in
481 stratospheric volcanic sulfate, *Geophys. Res. Lett.*, 30, doi: 10.1029/2003gl018134, 2003b.
482
483 Severi, M., Becagli, S., Traversi, R., and Udisti, R.: Recovering Paleo-Records from Antarctic Ice-Cores by Coupling a Continuous Melting
484 Device and Fast Ion Chromatography, *Analyt. Chem.*, 87, 11441-11447, doi: 10.1021/acs.analchem.5b02961, 2015.
485
486 Sigl, M., Toohey, M., McConnell, J. R., Cole-Dai, J., and Severi, M.: Volcanic stratospheric sulfur injections and aerosol optical depth
487 during the Holocene (past 11500 years) from a bipolar ice-core array, *Earth Syst. Sci. Data*, 14, 3167-3196, doi: 10.5194/essd-14-3167-2022,
488 2022.
489
490 Sigl, M., Winstrup, M., McConnell, J. R., Welten, K. C., Plunkett, G., Ludlow, F., Buntgen, U., Caffee, M., Chellman, N., Dahl-Jensen, D.,
491 Fischer, H., Kipfstuhl, S., Kostick, C., Maselli, O. J., Mekhaldi, F., Mulvaney, R., Muscheler, R., Pasteris, D. R., Pilcher, J. R., Salzer, M.,
492 Schupbach, S., Steffensen, J. P., Vinther, B. M., and Woodruff, T. E.: Timing and climate forcing of volcanic eruptions for the past 2,500
493 years, *Nature*, 523, 543-+, doi: 10.1038/nature14565, 2015.
494
495 Singarayer, J. S., Valdes, P. J., and Roberts, W. H. G.: Ocean dominated expansion and contraction of the late Quaternary tropical rainbelt,
496 *Scientific Reports*, 7, 9382, doi: 10.1038/s41598-017-09816-8, 2017.
497
498 Svensson, A., Bigler, M., Blunier, T., Clausen, H. B., Dahl-Jensen, D., Fischer, H., Fujita, S., Goto-Azuma, K., Johnsen, S. J., Kawamura,
499 K., Kipfstuhl, S., Kohno, M., Parrenin, F., Popp, T., Rasmussen, S. O., Schwander, J., Seierstad, I., Severi, M., Steffensen, J. P., Udisti, R.,
500 Uemura, R., Vallelonga, P., Vinther, B. M., Wegner, A., Wilhelms, F., and Winstrup, M.: Direct linking of Greenland and Antarctic ice
501 cores at the Toba eruption (74 ka BP), *Clim. Past*, 9, 749-766, doi: 10.5194/cp-9-749-2013, 2013.
502
503 Toohey, M. and Sigl, M.: Volcanic stratospheric sulfur injections and aerosol optical depth from 500 BCE to 1900 CE, *Earth Syst. Sci. Data*,
504 9, 809-831, doi: 10.5194/essd-9-809-2017, 2017.



505
506 Traversi, R., Becagli, S., Castellano, E., Marino, F., Rugi, F., Severi, M., Angelis, M. d., Fischer, H., Hansson, M., Stauffer, B., Steffensen,
507 J. P., Bigler, M., and Udisti, R.: Sulfate Spikes in the Deep Layers of EPICA-Dome C Ice Core: Evidence of Glaciological Artifacts,
508 *Environmental Science & Technology*, 43, 8737-8743, doi: 10.1021/es901426y, 2009.
509
510 Wallace, P. J. and Edmonds, M.: The Sulfur Budget in Magmas: Evidence from Melt Inclusions, Submarine Glasses, and Volcanic Gas
511 Emissions, *Reviews in Mineralogy and Geochemistry*, 73, 215-246, doi: 10.2138/rmg.2011.73.8, 2011.
512
513 Watt, S. F. L., Pyle, D. M., and Mather, T. A.: The volcanic response to deglaciation: Evidence from glaciated arcs and a reassessment of
514 global eruption records, *Earth-Sci. Rev.*, 122, 77-102, doi: 10.1016/j.earscirev.2013.03.007, 2013.
515
516 Wolff, E. W.: Electrical stratigraphy of polar ice cores: principles, methods, and findings. In: *Physics of Ice Core Records*, Hondoh, T. (Ed.),
517 Hokkaido University Press, Sapporo, 2000.
518
519 Wolff, E. W., Cook, E., Barnes, P. R. F., and Mulvaney, R.: Signal variability in replicate ice cores, *J. Glaciol.*, 51, 462-468, 2005.
520
521